Direct experimental observation of the single reflection optical Goos–Hänchen shift

H. G. L. Schwefel,[1,*] W. Köhler,[2] Z. H. Lu,[1] J. Fan,[3] and L. J. Wang[1]

[1]*Max-Planck Research Group, Institute of Optics, Information and Photonics, University of Erlangen-Nuremberg, Günther-Scharowsky-Straße 1, Bau 24, 91058 Erlangen, Germany*

[2]*FEMTOLASERS Produktions GmbH, Fernkomgasse 10, A-1100 Vienna, Austria*

[3]*Optical Technology Division, National Institute of Standards and Technology, 100 Bureau Drive, Mail Stop 8441, Gaithersburg, Maryland 20899, USA*

**Corresponding author: hschwefel@optik.uni-erlangen.de*

Received January 28, 2008; revised March 5, 2008; accepted March 5, 2008; posted March 11, 2008 (Doc. ID 92204); published April 9, 2008

We report a precise direct measurement of the Goos–Hänchen shift after one reflection off a dielectric interface coated with periodic metal stripes. The spatial displacement of the shift is determined by image analysis. A maximal absolute shift of 5.18 and 23.39 μm for TE and TM polarized light, respectively, is determined. This technique is simple to implement and can be used for a large range of incident angles. © 2008 Optical Society of America

OCIS codes: 260.6970, 240.6690, 110.2960.

When a beam of light is incident from a higher index material to a lower index dielectric it can undergo total internal reflection (TIR). Newton [1] predicted that the incident beam, in such a case, penetrates slightly into the lower index medium. Goos and Hänchen [2] postulated that such a penetration should lead the beam to laterally shift on the order of the wavelength. They were the first to measure such a shift, now known as the Goos–Hänchen (GH) shift [2]. The first theoretical description of the shift, for a plane wave, came from Artmann [3]:

$$D(\chi) = -\frac{\lambda}{2\pi}\frac{\mathrm{d}\phi}{\mathrm{d}\chi}, \tag{1}$$

where the displacement D is related to the phase change $\mathrm{d}\phi$ of the complex Fresnel reflection coefficient and the change of the incidence angle $\mathrm{d}\chi$. The wavelength in the denser medium is λ. Fresnel reflection laws show that the largest shift should occur at the onset of TIR, where Eq. (1) has a discontinuity. This discontinuity can be removed with a Gaussian ansatz, shown below in Eq. (2). As the Fresnel reflection coefficients differ for TE and TM polarization, a difference in the GH shift for TE and TM polarization is evident. It is this difference that has recently attracted great experimental interest [4–6]. Contrary to the original experiment 60 years ago, the current interest lies in measuring the GH shift after only one reflection. With the onset of negative index materials, predictions for negative GH shifts have also created theoretical interest [7,8]. "Regular" materials, however, still attract theoretical investigations, e.g., on curved surfaces [9], three-dimensional dome structures [10], and in active materials [11]. Proposed applications of the GH shift range from optical temperature sensing [12] to high-resolution surface plasmon sensors [13].

The experimental investigation of the GH shift in the optical regime has always been considered a relatively difficult task owing to the very small spatial shift, which at its maximum measures only a few wavelengths. Furthermore, choosing a good reference with which to measure the shift is a challenge. Recent experiments used the difference of the GH shift for TE and TM polarization and did not obtain an absolute value of the GH shift [4–6]. In this Letter, however, we report an experiment where we observe a direct measurement of the GH shift for the TE and the TM polarizations over a large range of incidence angles.

Goos and Hänchen [2] used multiple reflections in order to measure the spatial shift. They reasoned that owing to the high absorption of metals, light reflected from a metallic surface does not undergo a measurable spatial shift. There is a shift associated with thin metal films [8] and at grazing incidence [6]. This shift is, however, much smaller than that of the glass–air interface. In the GH setup, one beam is used to simultaneously reflect off the silver coating and the glass–air interface. Our experiment incorporated these ideas to measure the GH shift after only one reflection. Contrary to the original and the recent experiments, where polygonal prisms were used, we use a glass half-cylinder. A half-cylinder has the advantage of being able to couple light in from any angle of incidence. The planar side of the cylinder is coated with four metal stripes perpendicular to the cylinder axis, such that a collimated elliptical beam is incident on the glass–metal and the glass–air interface; see Fig. 1(a). The 0.5 mm wide metal stripes consisted of a 150 nm thick layer of chromium, which has a refractive index of $n_{\mathrm{Cr}}=3.537+4.362i$ (at 625 nm); see Fig. 1(c). This thickness ensures no unwanted interaction of the surface plasmon. A CCD camera images the reflected beam.

A partially coherent, 625 nm LED light source is used to minimize the distortion of speckles in the image. The polarization is selected by a sheet polarizer, and the beam is expanded with a telescope setup to ~7 mm. A cylindrical lens focuses the beam on a line to a width of 126 μm coinciding with the rotational axis of the half-cylinder. The BK7 half-cylinder, with refractive index of $n_{\mathrm{BK7}}=1.52$, is positioned on a rota-

 © 2008 Optical Society of America

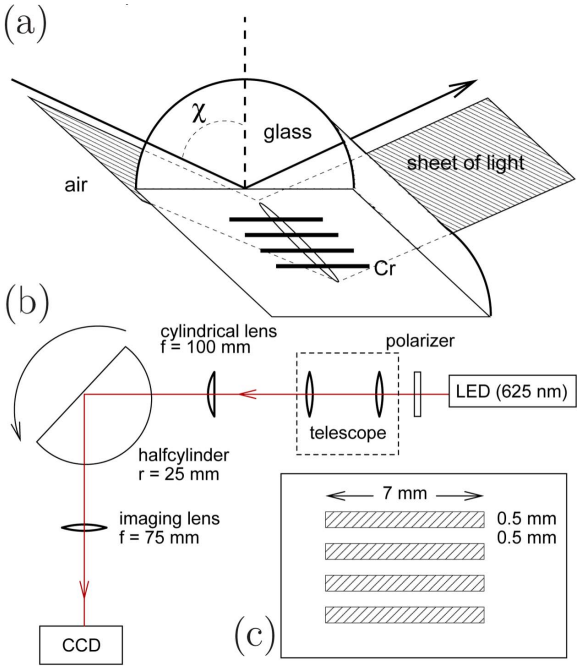

Fig. 1. (Color online) (a) Three-dimensional diagram of light impinging on the half-cylinder. (b) Schematic setup. (c) Configuration of the chromium stripes.

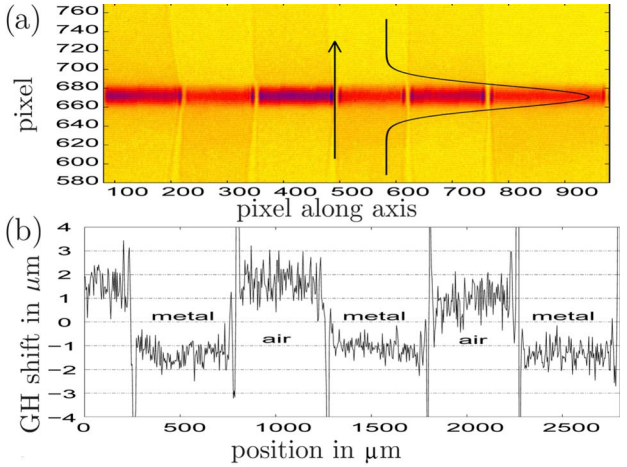

Fig. 2. (Color online) (a) CCD image for a TE polarized light incident at 39°. The stripes correspond to different reflection amplitudes at the glass–air and glass–metal interface. The arrow shows the direction in which the data are fitted by a Gaussian distribution. (b) Peak position of the fitted Gaussian with respect to the height on the cylinder (metal–air indicates the reflecting interface).

tional stage, around which the imaging lens and the detector can revolve. The CCD camera has 1024 $\times$2048 pixels, with a pixel size of 6.64 μm. Figure 1(b) shows a schematic of the setup, and Fig. 2(a) is a corresponding image of the reflected beam.

With a pixel size of 6.64 μm, the CCD camera cannot resolve the GH shift directly. Therefore, the data are fitted with a Gaussian profile along the direction of the arrow in Fig. 2(a). The width of the beam at the reflection point is ~20 pixels, which ensures a good Gaussian fit. This fitted peak and thus the central position of the reflected beam is calculated for each row of pixels perpendicular to the cylindrical axis and plotted in Fig. 2(b). The graph clearly shows a displacement of the reflected beam position between the glass–metal and the glass–air interface. To determine the shift, the boundary contributions are avoided by averaging the cental parts of Fig. 2(b). Rotating the half-cylinder and the detector, all angles of incidence can be scanned. The corresponding maximal GH shift is 5.18 μm for TE and 23.39 μm for TM. Figure 3 shows the experimental GH shift for both polarizations. Error bars are determined from the numerical fit of the Gaussian and statistical analysis. As the amplitude of the reflected light far below TIR ($\chi<41°$) is very close to the noise of the CCD, the error bars are considerably larger. At an angle between 37° and 41°, an early onset of the GH shift is observed.

Besides the limit of the critical angle, the limit of grazing incidence (80°–90°) has been of interest [14–16]. Analytically this limit is not well-understood, as the Gaussian optical approach is ill-suited in this limit, theoretical predictions go from vanishing to infinite shifts. Our experimental data show that the shift is small but finite at grazing incident. The recent publication of Merano *et al.* [6] sheds light on the small negative shift for the TM polarized light. We measure a finite $\approx$1 μm shift, which is in accordance with a negative GH shift for the metal, taking into consideration that the GH shift for the glass–air interface should be vanishing in that limit. However, at this limit the finite extent of the half-cylinder and the Gaussian beam come into effect, making the data less reliable.

Three theoretical approaches were used to understand our results. First, the plane-wave approximation of the field by Artmann [3] was used. Artmann's result is given in Eq. (1) and plotted with a solid curve in Fig. 3. In this limit the GH shift has a discontinuity at the critical angle, where the shift diverges. Second, the Gaussian wave approximation, analytically formulated by Horowitz and Tamir, [17] was used. The derived beam displacement, $D(\chi)$ is given by

$$D(\chi)=\frac{A(\chi)}{2^{5/4}\cos\chi}\mathrm{Re}\left[\sqrt{\frac{\omega}{k}}e^{i\pi/4}e^{\gamma_0^2/4}D_{-1/2}(\gamma_o)(1+A(\chi)[\sqrt{-\delta}-(2e^{i\pi}(k\omega)^{-2})^{1/4}e^{\gamma_0^2/4}D_{1/2}(\gamma_o)])^{-1}\right],$$

with

$$A(\chi)=4m\cos^2\chi_c\frac{\sin\chi}{\sqrt{\cos\chi(\sin\chi+\sin\chi_c)}[\cos^2\chi+m^2(\sin^2\chi-\sin^2\chi_c)]},$$

$$\delta=(\sin\chi-\sin\chi_c)\sec\chi,\quad \gamma_0=ink_0\delta\omega/\sqrt{2}, \tag{2}$$

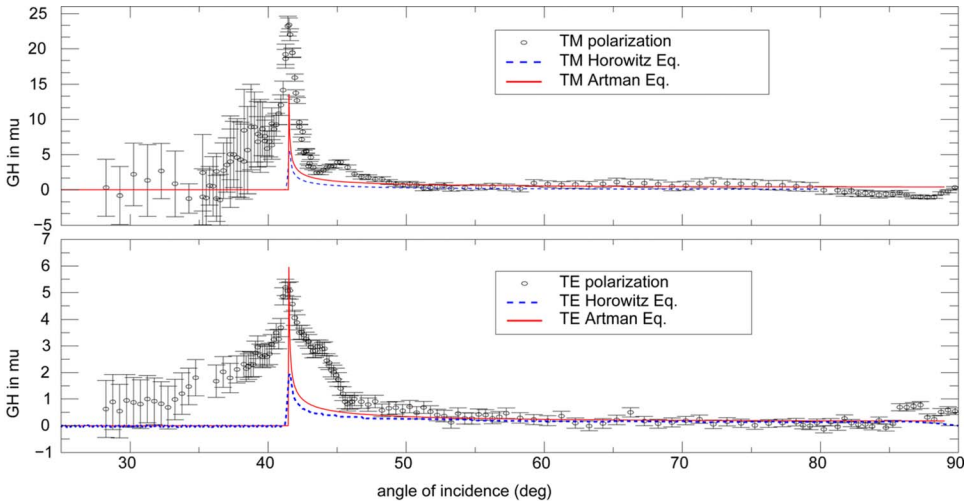

Fig. 3. (Color online) Goos–Hänchen shift for the TE and TM polarizations. The error bars for the experimental data are derived from the numerical fits and statistical analysis. Analytic descriptions of the shift have been included in the graph as shown in the legend. The solid curve (red online) corresponds to the plane wave ansatz of Artmann's Eq. (1). The dashed curve (blue online) corresponds to Horowitz's Gaussian ansatz Eq. (2).

where ω is the half-width of the beam; n is the index of refraction, $m=1$ for TE ($m=n^2$ for TM) polarization; k_0 is the wavenumber; $\chi_c=\arcsin 1/n$ is the critical angle; and $D_\nu(\gamma)$ is the parabolic-cylinder (or Weber) function of order ν and argument γ. This displacement is also shown in Fig. 3 (dashed curve), where a beam waist of $\omega=63$ μm is assumed. The discontinuity at the critical angle has been resolved and a broader shoulder of the GH shift is seen. Third, a numerical reflection of a Gaussian beam is simulated. The incident Gauss beam is Fourier transformed into the momentum space. In the momentum space Fresnel reflection laws are applied, and the beam is then inverse Fourier transformed. Back in real space the peaks of the incident and reflected beams are compared. The result coincides with the analytic results of Horowitz in the region of the critical angle and is therefore not plotted. Even the finite extent of the Gaussian beam calculations cannot explain the broadness of the measured GH shift. One reason for this could be that the partially coherent LED light source cannot be fully described by Gaussian optics [18]. We are investigating this effect for a future report.

In conclusion, we provide a novel experimental setup to directly measure the small lateral GH shift at TIR, for all angles of incidence. We report a maximum GH shift of 5.18 and 23.39 μm for TE and TM polarized light, respectively. For the first time, to the best of our knowledge, we measure the GH shift for all angles in the optical regime. Not only is this method fast, and provides a powerful image data analysis, but it is also inexpensive to set up.

The authors acknowledge stimulating discussions with G. Häusler and strong support from U. Peschel and Y. Cai.

References

1. I. Newton, *Opticks, or, A Treatise of the Reflections, Refractions, Inflections and Colours of Light* (Innys, 1718).
2. F. Goos and H. Hänchen, Ann. Phys. **1**, 333 (1947).
3. K. Artmann, Ann. Phys. **2**, 87 (1948).
4. F. Bretenaker, A. Le Floch, and L. Dutriaux, Phys. Rev. Lett. **68**, 931 (1992).
5. F. Pillon, H. Gilles, and S. Girard, J. Phys. IV **119**, 259 (2004).
6. M. Merano, A. Aiello, G. W. 't Hooft, M. P. van Exter, E. R. Eliel, and J. P. Woerdman, Opt. Express **15**, 15928 (2007).
7. I. V. Shadrivov, A. A. Zharov, and Y. S. Kivshar, Appl. Phys. Lett. **83**, 2713 (2003).
8. G. Dolling, M. W. Klein, M. Wegener, A. Schädle, B. Kettner, S. Burger, and S. Linden, Opt. Express **15**, 14219 (2007).
9. M. Hentschel and H. Schomerus, Phys. Rev. E **65**, 045603R (2002).
10. D. H. Foster, A. K. Cook, and J. U. Nöckel, Opt. Lett. **32**, 1764 (2007).
11. J. Fan and L. J. Wang, Opt. Commun. **259**, 149 (2006).
12. C.-W. Chen, W.-C. Lin, L.-S. Liao, Z.-H. Lin, H.-P. Chiang, P.-T. Leung, E. Sijercic, and W.-S. Tse, Appl. Opt. **46**, 5347 (2007).
13. X. Yin and L. Hesselink, Appl. Phys. Lett. **89**, 261108 (2006).
14. C. K. Carniglia, J. Opt. Soc. Am. **66**, 1425 (1976).
15. H. K. V. Lotsch, J. Opt. Soc. Am. **66**, 1426 (1976).
16. F. Pillon, H. Gilles, S. Girard, M. Laroche, and O. Emile, Appl. Phys. B **80**, 355 (2005).
17. B. R. Horowitz and T. Tamir, J. Opt. Soc. Am. **61**, 586 (1971).
18. L.-Q. Wang, L.-G. Wang, S.-Y. Zhu, and M. S. Zubairy, J. Phys. B **41**, 055401 (2008).